

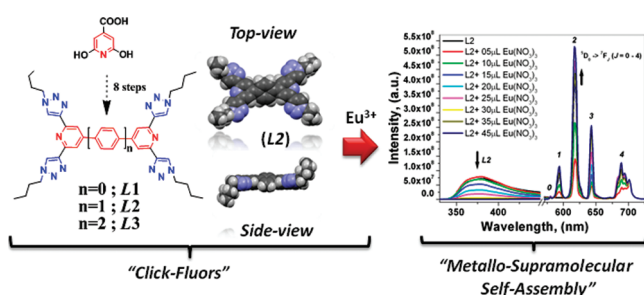
“Click-Fluors”: Synthesis of a Family of π -Conjugated Fluorescent Back-to-Back Coupled 2,6-Bis(triazol-1-yl)pyridines and Their Self-Assembly Studies

Naisa Chandrasekhar and Rajadurai Chandrasekar*

School of Chemistry, University of Hyderabad,
Prof. C. P. Rao Road, Gachhi Bowli, Hyderabad- 500046, India

rcsc@uohyd.ernet.in; chandrasekar100@yahoo.com

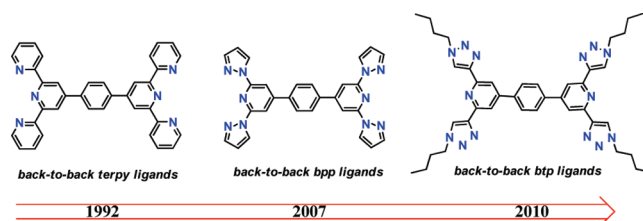
Received March 30, 2010



This paper presents an eight-step synthetic method for the preparation of a series of new back-to-back coupled 2,6-bis(triazol-1-yl)pyridine (btp) molecules (L1–L3). These L1–L3 molecules displayed fluorescent emission at 381, 381, and 457 nm, respectively. We also demonstrated the self-assembly of these fluorescent molecules with Eu^{3+} ions to obtain Eu^{3+} centered red-orange luminescent solids via “antenna effect”.

Nitrogen containing multitopic back-to-back (BTB) coupled 2,2':6',2''-terpyridine (BTB-terpy) and 2,6-bis-(pyrazolyl)pyridine (BTB-bpp) molecules have contributed immensely to the development of supramolecular chemistry,

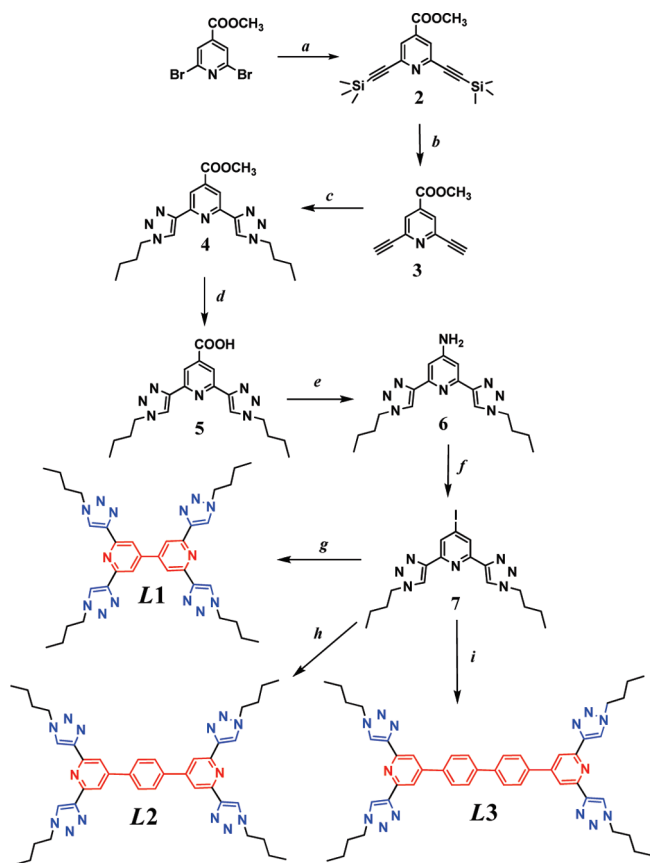
medicinal chemistry, bioinorganic chemistry, magnetochemistry, materials chemistry, and more recently in nanoscience and technology.^{1–6} A wide range of functional groups also can be introduced as substituents and used to control self-assembly processes and/or the properties of the complexes which result upon coordination to metal centers. Recently, the groups of Flood and Hecht^{5a,b} have independently introduced a new member to the tridentate ligand family, i.e., 2,6-bis(1,2,3-triazol-4-yl)pyridine (btp), synthesized via Sharpless click reaction condition.⁸ But until now, no multitopic BTB-btp derivatives have been synthesized in contrast to its structurally analogous counterparts, namely, BTB-terpy^{1g–i} and BTB-bpp,^{3b,7} due to the lack of reactive site on the readily accessible C-4 position of the pyridine unit. In contrast to both BTB-terpy and BTB-bpp, synthetically BTB-btp molecules offers tunable solubility provided by the readily available four alkyl chains obtained via Click chemistry (after 1,2,3-triazole ring formation). The emission range of the molecule also can be fine-tuned by varying π -conjugation lengths of the bridging units linking the two btp units.



Furthermore due to the presence of chelating tridentate N-donors in the front and back positions of L1–L3 they have the ability to shield Ln^{3+} ion completely from solvent molecules, especially water and alcohols, which are efficient

(1) (a) Lehn, J.-M. *Supramolecular Chemistry*; VCH: Weinheim, Germany, 1995. (b) Baxter, P. N. W. In *Comprehensive Supramolecular Chemistry*; Atwood, J. L., Davies, J. E. D., MacNicol, D. D., Vögtle, F., Eds.; Pergamon: Oxford, UK, 1996; p 165. (c) Schubert, U. S.; Hofmeier, H.; Newkome, G. R. *Modern Terpyridine Chemistry*; Wiley-VCH: Weinheim, Germany, 2006; p 69. (d) Hofmeier, H.; Schubert, U. S. *Chem. Soc. Rev.* **2004**, *33*, 373. (e) Balzani, V.; Scandola, F. *Supramolecular Photochemistry*; Horwood, E.: New York, 1991. (f) Constable, E. C. *Adv. Inorg. Chem. Radiochem.* **1986**, *30*, 69. (g) Constable, E. C.; Ward, M. D. *J. Chem. Soc., Dalton Trans.* **1990**, 1405. (h) Constable, E. C.; Thompson, A. J. *Chem. Soc., Dalton Trans.* **1992**, 3467. (i) Collin, J. P.; Lainé, P.; Launay, J.-P.; Sauvage, J.-P.; Sour, A. J. *Chem. Soc., Chem. Commun.* **1993**, 434. (j) Cargill Thompson, A. M. W. *Coord. Chem. Rev.* **1997**, *160*, 1. (k) Chelucci, G.; Thummel, R. P. *Chem. Rev.* **2002**, *102*, 3129. (l) Fallahpour, R.-A. *Synthesis* **2003**, 155. (m) Constable, E. C. *Chem. Soc. Rev.* **2007**, *36*, 246. (n) Pal, R. R.; Higuchi, M.; Kurth, D. G. *Org. Lett.* **2009**, *11*, 3562. (o) Han, F. S.; Higuchi, M.; Kurth, D. G. *Org. Lett.* **2007**, *9*, 559. (p) Kurth, D. G.; Lehmann, P.; Schutte, M. *Proc. Natl. Acad. Sci., U.S.A.* **2000**, *97*, 5704. (q) Han, F. S.; Higuchi, M.; Kurth, D. G. *J. Am. Chem. Soc.* **2008**, *130*, 2073. (r) Kurth, D. G.; Severin, N.; Rabe, J. P. *Angew. Chem., Int. Ed.* **2002**, *41*, 3681.

(2) (a) Halcrow, M. A. *Coord. Chem. Rev.* **2005**, *249*, 2880. (b) Halcrow, M. A. *Coord. Chem. Rev.* **2009**, *253*, 2493. (3) (a) Rajadurai, C.; Schramm, F.; Brink, S.; Fuhr, O.; Kruk, R.; Ghafari, M.; Ruben, M. *Inorg. Chem.* **2006**, *45*, 10019. (b) Rajadurai, C.; Fuhr, O.; Kruk, R.; Ghafari, M.; Hahn, H.; Ruben, M. *Chem. Commun.* **2007**, 2636. (c) Rajadurai, C.; Qu, Z.; Fuhr, O.; Balaji, G.; Kruk, R.; Ghafari, M.; Ruben, M. *Dalton Trans.* **2007**, 3531. (d) Chandrasekar, R.; Schramm, F.; Fuhr, O.; Ruben, M. *Eur. J. Inorg. Chem.* **2008**, *17*, 2649. (4) (a) Bunzli, J.-C. G.; Piguet, C. *Chem. Soc. Rev.* **2005**, *34*, 1048. (b) Kadjane, P.; Starck, M.; Camerel, F.; Hill, D.; Hildebrandt, N.; Ziessel, R.; Charbonnière, L. *J. Inorg. Chem.* **2009**, *48*, 4601. (5) (a) Li, Y.; Huffmana, J. C.; Flood, A. H. *Chem. Commun.* **2007**, 2692. (b) Meudtner, R. M.; Ostermeier, M.; Goddard, R.; Limberg, C.; Hecht, S. *Chem.—Eur. J.* **2007**, *13*, 9834. (c) Meudtner, R. M.; Hecht, S. *Macromol. Rapid Commun.* **2008**, *29*, 347. (d) Li, Y.; Flood, A. H. *Angew. Chem., Int. Ed.* **2008**, *47*, 2649–2652. (e) Li, Y.; Flood, A. H. *J. Am. Chem. Soc.* **2008**, *130*, 12111. (f) Li, Y.; Pink, M.; Karty, J. A.; Flood, A. H. *J. Am. Chem. Soc.* **2008**, *130*, 17293. (g) Meudtner, R. M.; Hecht, S. *Angew. Chem., Int. Ed.* **2008**, *47*, 4926. (h) Juwarker, H.; Lenhardt, J. M.; Pham, D. M.; Craig, S. L. *Angew. Chem., Int. Ed.* **2008**, *47*, 3740. (i) Juwarker, H.; Lenhardt, J. M.; Castillo, J. C.; Zhao, E.; Krishnamurthy, S.; Jamiolkowski, R. M.; Kim, K.-H.; Craig, S. L. *J. Org. Chem.* **2009**, *74*, 8924. (6) Chandrasekhar, N.; Chandrasekar, R. *Chem. Commun.* **2010**, 46, 2915. (7) Basak, S.; Hui, P.; Chandrasekar, R. *Synthesis* **2009**, 23, 4042. (8) (a) Rostovtsev, V. V.; Green, L. G.; Fokin, V. V.; Sharpless, K. B. *Angew. Chem., Int. Ed.* **2002**, *41*, 2596. (b) Chan, T. R.; Hilgraf, R.; Sharpless, K. B.; Fokin, V. V. *Org. Lett.* **2004**, *6*, 2853.

SCHEME 1. Synthetic Route to Back-to-Back Coupled 2,6-Bis-(triazol-1-yl)pyridine Ligands (**L1**–**L3**)^a

^aReagents and conditions: (a) TMSA/[Pd(PPh₃)₄]/CuI/THF/(C₂H₅)₃N/4 h/rt; (b) KF/methanol/30 min/rt; (c) butylazide/sodium ascorbate/copper(II) sulfate pentahydrate/10 h/rt; (d) LiOH/THF/HCl (2 N); (e) C₂O₂Cl₂/NaN₃/TFA/K₂CO₃; (f) NaNO₂/HCl/aqueous KI; (g) [Pd(PPh₃)₄]/bispinacalatodiboron/DMF/K₂CO₃/3 d/70 °C; (h) [Pd(PPh₃)₄]/1,4-phenylenebisdiboronic acid/1,4-dioxane/Na₂CO₃/3 d/70 °C; (i) [Pd(PPh₃)₄]/4,4'-biphenyldiboronic acid/1,4-dioxane/Na₂CO₃/3 d/70 °C.

quenchers of Ln³⁺ luminescence.⁵ It is also expected that the significant absorption of **L1**–**L3** in the UV region might help to antennae their excitation energy efficiently to the excited state(s) of the Ln³⁺ ions to obtain sensitized light emission. This is in fact useful to design and fabricate efficient photonic devices based on Ln³⁺ complexes. Moreover due to the BTB coupled orientation of each btp unit in **L1**–**L3**, they are expected to form rare Eu³⁺ containing luminescent 3D metallo-supramolecular networks [(Ln(**L1** or **L2** or **L3**))₃]³⁺_n via self-assembly.

In this paper, for the first time, we report our novel methodology for the synthesis of a series of π -conjugated fluorescent (solution and solid state) BTB coupled btp molecules **L1**–**L3** (without bridging unit ($n = 0$), with phenyl ($n = 1$), and biphenyl ($n = 2$) bridging units, respectively; where n is the number of phenyl linkers), their characterizations, the crystal structure of **L2**, and their potential use in preparing luminescent solids via self-assembly with Eu³⁺ metal ion.

For the synthesis of BTB coupled btp (**L1**–**L3**) molecules, a new eight-step synthetic protocol from the low-priced citrazinic acid was developed (Scheme 1). Transformation of citrazinic acid into 2,6-dibromoisonicotinic acid methyl

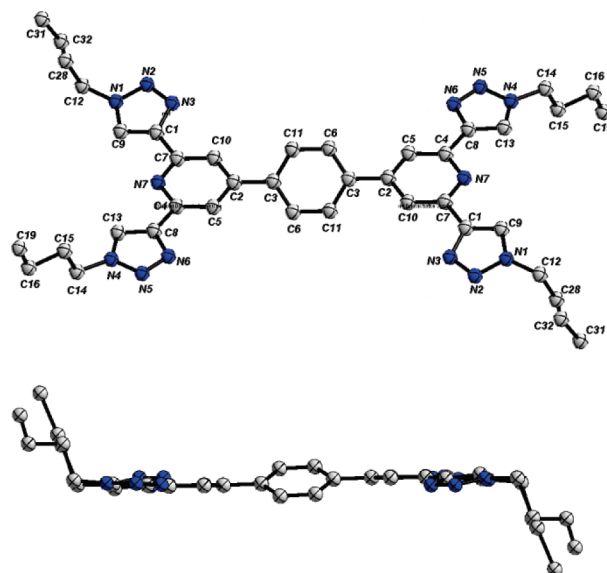


FIGURE 1. ORTEP diagram of **L2** at 293 K with atomic labels (top figure) and its side view (bottom figure). Hydrogen atoms are omitted for clarity.

ester was effected as reported.⁹ Conversion of 2,6-dibromoisonicotinic acid methyl ester into **2** was effected in 72% yield via Sonogashira coupling conditions by using trimethylsilylacetylene (TMSA) and Pd(PPh₃)₄ catalyst in Et₃N/THF. Deprotection of **2** in the presence of MeOH/KF gave the 2,6-diethynyl Click precursor **3** in a quantitative 99% yield. Formation of five-member triazole units was effected on **3** by using Click reaction conditions with Cu(SO₄)₂/sodium ascorbate in the presence of butylazide to synthesize the ester derivative of btp **4** in 97% yield. The saponification reaction quantitatively converted **4** into its carboxylic acid derivative **5** in 98% yield. Furthermore, sequential conversion of the carboxylic acid in **5** into acyl azide followed by a thermal Curtius rearrangement and succeeding hydrolysis of the trifluoroacetamide provided the amino derivative **6** in 78% yield as a white powder. From this compound **6**, the 4-iodo-2,6-ditriazolylpyridine **7** was synthesized in a modest 36% yield by diazotization and followed by reaction with KI. Treatment of compound **7** with bispinacalatodiboron under Suzuki cross-coupling condition formed a directly BTB coupled btp **L1** in a decent 41% yield. Suzuki cross-coupling reactions of compound **7** with 1,4-phenyldiboronic acid and 4,4'-biphenyldiboronic acid provided the target molecules **L2** and **L3** in ca. 50% yield. The structures of the molecules **L1**–**L3** were characterized unambiguously by ¹H and ¹³C NMR, LCMS, and elemental analyses (see the Supporting Information). Compound **L2** was successfully crystallized as colorless plates in chloroform by slow evaporation technique.

Single-crystal X-ray analysis of **L2** revealed the monoclinic P2(1)/c space group (Figure 1). The molecule is near planar and the torsion angle between the bridging phenyl ring and the pyridine unit is 26.28° (C5–C2–C3–C6). The N7···N7' distance between the two pyridine units is 1.13 nm. Per unit cell four molecules of **L2** were found. In **L2** the two triazole rings in the btp cores adopt *anti-anti* conformation due to the repulsive interaction of the lone pairs of the ring

(9) Amb, C. M.; Rasmussen, S. C. *J. Org. Chem.* **2006**, *71*, 4696.

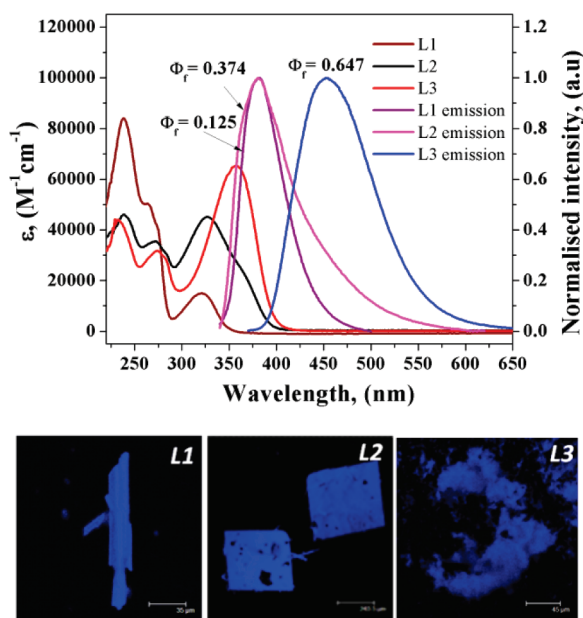


FIGURE 2. Top: UV-vis absorbance and emission properties of L1–L3 in DCM. Bottom: Confocal fluorescence microscope images of L1–L3.

TABLE 1. Photophysical Properties of L1–L3 in Dichloromethane

compd	λ_{abs} [nm] (ϵ [$\text{M}^{-1} \text{cm}^{-1}$])	$\lambda_{\text{emission}}$ [nm]	Φ_f^a
L1	265 (50167); 319 (15164)	381	0.125
L2	271 (35445); 327 (45104)	381	0.374
L3	274 (31754); 358 (65582)	457	0.647

^aQuinine sulfate as reference ($Q_{\text{ref}} = 0.577$) and excitation at 331 nm for all samples.

nitrogen atoms (N2, N7, and N5) and C–H...N hydrogen bonding interactions.⁵ The UV-vis absorption studies of L1–L3 in DCM displayed absorption maxima at λ_{max} 319, 327, and 358 nm, respectively (Figure 2). Both L1 and L2 showed a violet fluorescence with emission maxima at $\lambda_{\text{max}} = 381$ nm ($\lambda_{\text{ex}} = 291$ nm), while L3 exhibited a red-shifted blue emission at $\lambda_{\text{max}} = 457$ nm ($\lambda_{\text{ex}} = 358$ nm). The quantum yield (Φ_f) of L1–L3 increased in the following order: 0.125, 0.374, and 0.647, respectively. Interestingly, L1–L3 showed remarkable fluorescence also in the solid states (powder, crystalline), when exposed to 365 nm UV light (Table 1).

The self-assembly efficiency of L2 and L3 was examined with Eu^{3+} ions. The corresponding luminescent property of the self-assembled product was also investigated. For example, treatment of $\text{Eu}(\text{NO}_3)_3$ with a 3-fold excess of ligands L2 formed an air stable complex $[\text{Eu}(\text{L2})_3(\text{NO}_3)_3]_n$ **1** as a white precipitate, which exhibits red-orange fluorescent under UV light ($\lambda_{\text{ex}} = 365$ nm). The ^1H NMR spectrum of the soluble smaller fragments of complex **1** in $\text{CD}_3\text{CN}-d_3$ solvent showed substantial broadening and informal paramagnetic shifted NMR peaks (Supporting Information, Figure S3). Interestingly, the aromatic region of the spectra showed three peaks for L2 and four peaks for **1**. An additional paramagnetically shifted peak in the aromatic region of **1** possibly arises from the resonance of the uncoordinated btp core protons of the 3D polymer chain ends. The aliphatic region of the spectrum of **1** further supported this observation by exhibiting several paramagnetically shifted alkyl chain proton peaks due to an efficient spin density propagation from the Eu^{3+}

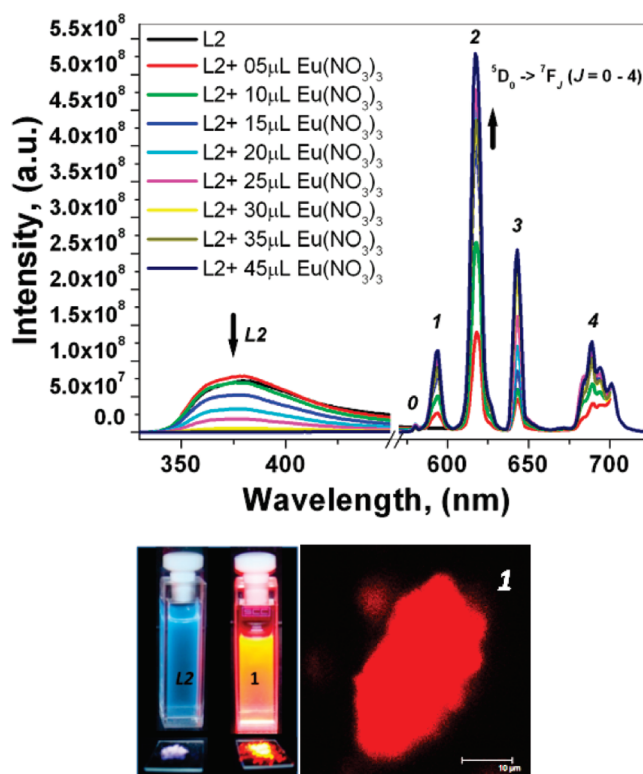


FIGURE 3. Top: UV-vis emission changes during the titration of L2 ($c = 1.053 \times 10^{-5}$ M; DCM) with $\text{Eu}(\text{NO}_3)_3$ solution ($c = 0.72 \times 10^{-3}$ M; ACN). The arrow facing down (\downarrow) shows the decreasing fluorescent intensity of the ligand and the arrow facing up (\uparrow) shows the increasing Eu^{3+} emission. Bottom: Solution and solid state emission of L2 and **1**.

ion to the alkyl chains, in addition to the unshifted alkyl chain proton peaks of the uncoordinated terminal btp cores (no spin density delocalization). Since the bulk of the compound of **1** is not soluble in the same acetonitrile solvent, compound that remains insoluble is supposed to represent 3D higher chain homologues. It is evident from the recent examples that the monomeric btp ligand formed a nine-coordinated Eu^{3+} complex with a trigonal prismatic geometry.^{5a,b} On the basis of this report, it is anticipated that **1** also adopts a similar type of coordination environment with 3D polymeric nature $[\text{Eu}(\text{L2})_3(\text{NO}_3)_3]_n$.

In the photoluminescence studies (Figure 3), compound **1** exhibited highly red-orange luminescence under UV light both in the powder state and in solution. Titration of an acetonitrile solution of $\text{Eu}(\text{NO}_3)_3$ with a DCM solution of L2 showed a gradual decrease of the ligand fluorescence and enhancement of complex **1** emission bands. The complete disappearance of the broad violet emission band observed at 381 nm for L2 indicated the completion of metal–ligand self-assembly. The ligand centered excitation produced Eu^{3+} centered $^5\text{D}_0 \rightarrow ^7\text{F}_J$ ($J = 0-4$) emission bands for **1**. This observation points out an efficient ligand–to–metal energy transfer process called the “antenna effect”. The emission spectra are typical of species with low metal ion site symmetry, and they are dominated by the hypersensitive $^5\text{D}_0 \rightarrow ^7\text{F}_2$ transition.

In conclusion we presented a novel eight-step synthetic protocol for the preparation of three back-to-back coupled btp molecules L1–L3. The solid state structure of the ligand L2

showed the near planar structure and adoption of *anti-anti* conformation of the btp units. Interestingly molecules **L1–L3** displayed light violet, violet, and blue fluorescence, respectively, in the solid state (powder and crystal) and in solution due to the different π -conjugation lengths. Due to the ditopic nature of the ligand **L2**, it self-assembled efficiently with Eu^{3+} ions forming a red-orange (solid and solution state) emitting **1**. This was further supported by the $f \leftrightarrow f$ transitions in the UV–vis region. Detailed photophysical properties are under investigation.

Experimental Section

2,6-Bis(1-butyl-1*H*-1,2,3-triazol-4-yl)-4-iodopyridine (7), 2,6-Bis(1-butyl-1*H*-1,2,3-triazol-4-yl)pyridin-4-amine (**6**) (0.075 g, 0.22 mmol, 1.0 equiv) was suspended in concd HCl (5 mL) and stirred for 24 h at rt. The mixture was cooled in an ice bath and NaNO_2 (0.032 g, 0.44 mmol, 2.0 equiv) dissolved in a minimum amount of water (1 mL) was added dropwise. To this KI in water (5 mL) was slowly added and the solution was stirred for 5 min. THF (10 mL) was added into the reaction mixture and the solution was neutralized by adding solid NaHCO_3 . The product was extracted with ether and washed with $\text{Na}_2\text{S}_2\text{O}_3$ solution. The collected organic layers were dried over MgSO_4 and the solvent was evaporated on a vacuum evaporator to obtain a pale yellow crude product, which upon washing with petroleum ether gives **7** as white color powder in 36% yield (0.037 g). ^1H NMR (400 MHz, CDCl_3) δ 8.49 (s, 2H), 8.13 (s, 2H), 4.44 (t, $^3J = 7.64$ Hz, 4H), 1.96 (q, $^3J = 7.64$ Hz, 4H), 1.45–1.36 (m, 4H), 0.98 (t, $^3J = 7.35$ Hz, 6H). ^{13}C NMR (100 MHz, CDCl_3) δ 150.5, 147.1, 128.3, 122.3, 106.9, 50.4, 32.3, 19.8, 13.6. LC-MS m/z calcd 451.25, found 451.10. Anal. Calcd for $\text{C}_{17}\text{H}_{22}\text{IN}_7$: C, 45.24; H, 4.91; N, 21.73. Found: C, 45.10; H, 4.85; N, 21.87.

2,2',6,6'-Tetrakis(1-butyl-1*H*-1,2,3-triazolyl)-4,4'-bipyridine (L1). Compound **7** (0.10 g, 0.221 mmol), bispinacalotodiboron (0.061 g, 0.24 mmol), K_2CO_3 (0.092 g, 0.665 mmol), and $[\text{Pd}(\text{PPh}_3)_4]$ (0.018, 0.016 mmol, 0.05 equiv) were suspended in degassed DMF (30 mL). The reaction mixture was heated at 70 °C for 3 d under nitrogen atmosphere. The course of the reaction was monitored by TLC (1:19 methanol:DCM). After disappearance of the starting material the reaction mixture was cooled to rt and then DMF was removed with a rotary evaporator. The resulting residue was treated with water and extracted with CH_2Cl_2 solvent. The separated organic layer was dried over MgSO_4 and the solvent was removed on a rotary evaporator. The yellow residue was obtained and purified by column chromatography (silica, 1:50 methanol:DCM). The obtained first fraction was collected, and rotary evaporated to afford **L1** as a white powder in 41% yield (0.059 g). UV–vis (CH_2Cl_2) λ_{abs} (ϵ) 265 (50167), 319 (15164); λ_{emis} 381. ^1H NMR (400 MHz, CDCl_3) δ 8.50 (s, 4H, 5'), 8.25 (s, 4H, 3), 4.46 (t, $^3J = 7.06$ Hz, 8H, 1''), 1.98 (q, $^3J = 7.32$ Hz, 8H, 2''), 1.46–1.36 (m, $^3J = 7.57$ Hz, 8H, 3''), 0.99 (t, $^3J = 7.32$ Hz, 12H, 4''). ^{13}C NMR (100 MHz, CDCl_3) δ 150.3, 148.1, 147.6, 122.3, 117.3, 50.4, 32.4, 19.8, 13.6. LC-MS m/z calcd 648.81, found 648.90.

1,4-Bis(1,2':6',1''-bis(3-butyl-1*H*-3,4,5-triazolyl)pyridin-4'-yl)-benzene (L2). Compound **7** (0.14 g, 0.31 mmol), 1,4-phenylenebisboronic acid (0.028 g, 0.16 mmol), and $[\text{Pd}(\text{PPh}_3)_4]$ (0.018,

0.016 mmol, 0.05 equiv) were suspended in degassed 1,4-dioxane (30 mL). Na_2CO_3 (2 M, 5 mL) was added to the mixture and heated at 70 °C for 3 d under nitrogen atmosphere. The course of the reaction was monitored by TLC (1:19 methanol:DCM). After disappearance of the starting material the reaction mixture was cooled to rt and then 1,4-dioxane was removed with a rotary evaporator. The resulting residue was treated with water and extracted with CH_2Cl_2 solvent. The separated organic layer was dried over MgSO_4 and the solvent was removed on a rotary evaporator. The orange residue was washed with a small amount of petroleum ether (bp 60 °C) to remove the colored impurities and to afford compound **L2** as a white powder in 48% yield (0.105 g). UV–vis (CH_2Cl_2) λ_{abs} (ϵ) 271 (35445), 327 (45104); λ_{emis} = 381. ^1H NMR (400 MHz, CDCl_3) δ 8.46 (s, 4H, 5'), 8.26 (s, 4H, 3), 8.04 (s, 4H, 2''), 4.47 (t, $^3J = 7.26$ Hz, 8H, 1''), 1.97 (q, $^3J = 7.46$ Hz, 8H, 2''), 1.46–1.36 (m, 8H, 3''), 0.99 (t, $^3J = 7.36$ Hz, 12H, 4''). ^{13}C NMR (100 MHz, CDCl_3) δ 150.7, 149.2, 148.3, 138.7, 127.1, 127.1, 117.0, 50.3, 32.3, 19.7, 13.5. FTIR (KBr disk; ν in cm^{-1}) 3483, 2928, 1612, 1460, 1381, 1041, 790. LC-MS m/z calcd 723.90, found 724.42. Anal. Calcd for $\text{C}_{40}\text{H}_{48}\text{N}_{14}$: C, 66.27; H, 6.67; N, 27.05. Found: C, 66.17; H, 6.71; N, 26.85.

4''',4''-(Biphenylene)bis(2,6-bis(1-butyl-1*H*-1,2,3-triazol-4-yl)-pyridine (L3). Compound **7** (0.090 g, 0.2 mmol), 4,4'-diphenylenebisboronic acid (0.24 g, 0.095 mmol), and $[\text{Pd}(\text{PPh}_3)_4]$ (0.012 g, 0.01 mmol) were suspended in degassed 1,4-dioxane (30 mL). Na_2CO_3 (2 M, 5 mL) was added and the mixture was heated at 70 °C for 3 d under nitrogen atmosphere. The course of the reaction was monitored by TLC (1:19 methanol:DCM). After disappearance of the starting material the reaction mixture was cooled to rt and then 1,4-dioxane was removed with a rotary evaporator. The resulting residue was treated with water and extracted with CH_2Cl_2 solvent. The separated organic layer was dried over MgSO_4 and the solvent was removed on a rotary evaporator. The orange residue was washed with a small amount of petroleum ether to remove the colored impurities and to afford compound **L2** as a white powder in 51% yield (0.082 g). UV–vis (CH_2Cl_2) λ_{abs} (ϵ) 274 (31754), 358 (65582); λ_{emis} = 457. ^1H NMR (400 MHz, CDCl_3) δ 8.45 (s, 4H, 5'), 8.230 (s, 4H, 3), 7.99 (dd, 8H, 2''), 7.84 (dd, 8H, 3''), 4.48 (t, $^3J = 7.38$ Hz, 8H, 1''), 2.20 (q, $^3J = 7.60$ Hz, 8H, 2''), 1.47–1.37 (m, 8H, 3''), 1.01 (t, $^3J = 7.38$ Hz, 12H, 4''). ^{13}C NMR (100 MHz, CDCl_3) δ 150.8, 149.6, 148.5, 146.2, 127.8, 122.15, 117.0, 50.4, 32.4, 19.8, 13.5. FTIR (KBr disk; ν in cm^{-1}) 3123, 2959, 2930, 2866, 1703, 1614, 1568, 1458, 1379, 1205, 1043, 821. LC-MS m/z calcd 801.10, found 801.00. Anal. Calcd for $\text{C}_{46}\text{H}_{52}\text{N}_{14}$: C, 68.98; H, 6.54; N, 24.48. Found: C, 68.87; H, 6.49; N, 24.35.

Acknowledgment. We are grateful to DST (Fast Track Scheme No. SR/FTP/CS-115/2007), New Delhi for financial support. N.C. thanks CSIR for a JRF fellowship.

Supporting Information Available: General experimental methods, synthesis of (**1–6**), characterization data (**2–7**, **L1–L3**), crystallographic data/CIF file of **L2** and UV–vis absorption/fluorescent titration data of **L3** with $\text{Eu}(\text{III})$. This material is available free of charge via the Internet at <http://pubs.acs.org>.